Original Research Report

Mouse Embryonic Stem Cell-Derived Spheres with Distinct Neurogenic Potentials

ANNALENA MOLINER,[1] PATRIK ENFORS,[2] CARLOS F. IBÁÑEZ,[1] and MICHAEL ANDÄNG[2]

ABSTRACT

Mouse embryonic stem (ES) cells grown in feeder-free suspension cultures in the presence of leukemia inhibitory factor (LIF) and basic fibroblast growth factor (bFGF) form spheres that retain pluripotency after multiple passages. ES cell-derived spheres of any passage acquired increased competence to differentiate into neurons over time in culture. Eight-day-old spheres produced many neurons upon plating in differentiation conditions whereas 3-day-old spheres produce none, even after monolayer expansion or treatment with blockers of inhibitory signals, indicating the acquisition of a reversible, proto-neurogenic state during sphere development. Gene expression profiling with oligonucleotide microarrays was used to identify the transcriptional changes accompanying this process. Sphere growth was characterized by down-regulation of a subset of ES cell-expressed genes during the first few days of sphere formation, and progressive up-regulation of novel genes over the course of 1 week in culture. Differential gene expression between 3-day-old and 8 day-old spheres was verified by quantitative real-time PCR experiments. Gene Set Enrichment Analysis (GSEA) of microarray data indicated that neurogenic potential in the late stages of sphere development correlated predominantly with up-regulation of pathways related to mitochondrial function, cell metabolism, oxidative stress, hypoxia, and down-regulation of RNA transcription and proteasome machineries, as well as pathways induced by myc and repressed by retinoic acid. We propose that differences in cellular metabolic state brought about by cell–cell contact and paracrine interactions in the sphere niche may play crucial roles in biasing the early stages of ES cell differentiation toward a neuronal phenotype.

INTRODUCTION

THE CAPACITY OF EMBRYONIC STEM (ES) CELLS to self-renew and generate cell types from any of the three embryonic germ layers has attracted enormous interest, both for their possible use in the production of differentiated cell types for regenerative medicine and as a model of embryonic development. Understanding the genetic programs that govern ES cell maintenance and differentiation into specific cell types has implications for both basic cell biology and the potential clinical applications of ES cells. Gene expression profiles in ES cells and more tissue-restricted stem cell types, such as hematopoietic and neural stem cells (NSCs), have been investigated rather extensively in recent years. Although some studies have been devoted to comparing expression profiles of ES and NSCs [1–3], much less is known about the intermediate stages that are likely to exist along the lineage that connects those two stem cell populations.

Mouse ES cells are derived from the inner cell mass (ICM) of the preimplantation embryo and can be grown and maintained in an undifferentiated state in vitro in the

[1]Department of Neuroscience, and [2] Department of Medical Biochemistry and Biophysics, Karolinska Institute, 17177 Stockholm, Sweden.

presence of serum, leukemia inhibitory factor (LIF), and a feeder layer of mitotically inactive mouse embryonic fibroblast (MEF) cells. ES cells grown at low density have the capacity to generate floating sphere-like clonal colonies in the absence of feeder cells or serum, but in the presence of LIF [4,5]. Interestingly, when plated under conditions favorable to neural differentiation, ES cell-derived spheres are capable of generating neurons, astrocytes, and oligodendrocytes [4], indicating that neural competence can be induced in ES cells during sphere culture. Sphere cells retain some nonneural properties, and, unlike bona fide NSCs, they can contribute extensively to all tissues in chimeric mice [4]. For this reason, they have been called "primitive neural stem cells" by some researchers [4]. LIF-dependent, sphere-forming cells with similar properties have also been isolated from the epiblast of mouse embryos [6].

The original conditions used to generate sphere colonies from mouse R1 ES cells included, in addition to LIF and basic fibroblast growth factor (bFGF), B27 supplement, which is thought to prevent cell death by inhibiting free-radical induced damage [4]. However, this supplement is also known to contain high levels of retinol [7], which ES cells can readily convert into retinoic acid (RA) [8], a well-known neural-differentiating agent [9]. In this study, we describe the neurogenic potential of sphere cultures derived from D3 and R1 mouse ES cell lines in the presence of LIF, bFGF, and N2 medium, but without B27 supplement. Dissociated 8-day-old spheres derived in these conditions remain pluripotent [5], and can be used for the efficient propagation of ES cells in feeder-free suspension cultures. In the present study, we show that spheres derived from ES cells in N2 medium acquire neurogenic potential over time in culture. In addition, we have used Affymetrix oligonucleotide microarrays to elucidate the genome-wide transcriptional changes that underlie the formation of ES cell-derived spheres and the acquisition of neurogenic competence by these cells.

MATERIALS AND METHODS

Growth of ES cells and ES cell-derived spheres

ES cells were grown over a monolayer of MEF cells mitotically inactivated by γ-irradiation (2,500 rad) in knockout Dulbecco's modified Eagle medium (KO-DMEM; Invitrogen) supplemented with 10% KO Serum Replacement (Gibco), 100 mM sodium pyruvate (Gibco), nonessential amino acids (Gibco), 50 μM β-mercaptoethanol, Glutamax (Gibco), and 1,000 U/ml LIF (ESGRO, Chemicon). ES cells were isolated free from MEF contamination by taking the following precautions (see also ref. 3): (1) ES cell colonies were detached after very mild dissociation with Tryp Express (Gibco), a condition under which most MEFs remained attached to the dish; (2) cells were incubated for 40 min at 37°C in a fresh dish, so that any remaining MEFs

selectively adhered to the bottom; (3) the supernatant of the dish was collected and cells were reincubated for another 10 min at 37–C in a fresh dish. No MEFs were observed at this stage. ES cells were recovered from the supernatant and lysed in the RLT reagent (Qiagen) for RNA isolation (see below).

ES cell-derived spheres were grown in suspension in T175 flasks in DMEM/F12 50/50, 10 mM HEPES, and 50 μM β-mercaptoethanol supplemented with N2 (Invitrogen), 10 ng/ml bFGF (R&D Systems), and 1,000 U/ml of LIF (ESGRO, Chemicon). For passage after 6–10 days, cells were dissociated with 1 mg/ml collagenase/dispase in PBS (Roche) and seeded at a density of $5 - 10 \times 10^3$ cells/ml.

Flow cytometry

Cells were dissociated and incubated in primary antibody against stage-specific embryonic antigen-1 (SSEA-1, 1:400) in phosphate-buffered saline (PBS) including 1% bovine serum albumin (BSA) (Developmental Studies Hybridoma Bank) for 1 h at 4°C followed by incubation in fluorescein isothiocyanate (FITC)-conjugated secondary antibody (1:400; Jackson Immuno Research) for 1 h at 4°C followed by incubation in PBS with 1% BSA and 1 mg/ml propidium iodide (PI; Sigma) to discriminate dead cells. Negative controls were treated identically but without primary antibody.

Neuronal differentiation and immunocytochemistry

For ES cell differentiation, 24-well cell culture plates were coated with 500 μg/ml poly-D-lysine for 15 min followed by 20 mg/ml of mouse laminin 1 (Invitrogen) for at least 4 h. Spheres were plated in 0.5–1 ml of minimum essential medium (MEM), F-12 50/50, HEPES, and β-mercaptoethanol, supple-
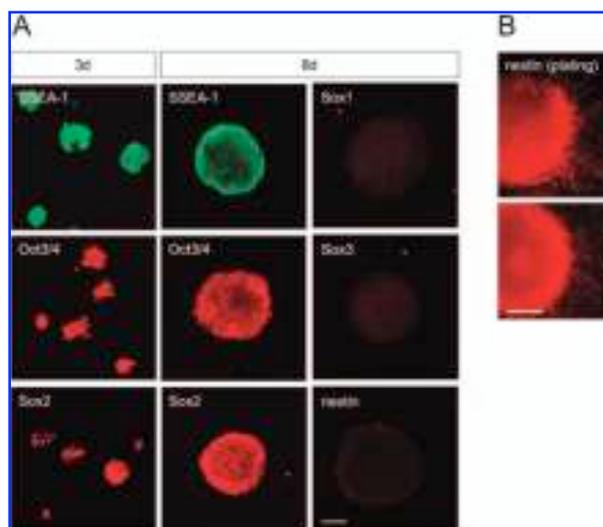
FIG. 1. Characterization of 3d and 8d ES cell-derived spheres. (**A**) Analysis of expression of ES cell markers SSEA-1, Oct-3/4, and Sox2 and NSC markers Sox1, Sox3, and nestin in 3d and 8d ES cell-derived spheres. Size bar, 50 μm. (**B**) Nestin expression in 8d spheres after overnight plating on poly-D-lysine coated dishes. Size bar, 50 μm.

mented with N2. The medium was changed after 2–3 days. After 5 days of differentiation, 20 ng/ml glial cell-derived neurotrophic factor (GDNF; R&D), 20 ng/ml bone-derived neurotrophic factor (BDNF; R&D), and 50 ng/ml nerve growth factor (NGF; Promega) was added to the medium. For immunocytochemistry, cells, either adherent or as spheres in suspension, were fixed in 4% paraformaldehyde/PBS for 20 min and washed and blocked for 30 min in PBT buffer (PBS, 0.3% Triton X-100, 1% BSA). Primary antibodies were diluted in PBT (SSEA-1, 1:400; Developmental Studies Hybridoma Bank; Sox1, Sox2 and Sox3, 1:400, Chemicon; βIII tubulin, 1:400, Promega; nestin, 1:1,000, Chemicon) and incubated overnight at 4°C. Secondary antibodies (Alexa Fluor 488 or 555 conjugated, Invitrogen) were diluted 1:800 in PBS and 1% BSA and incubated for 2 h followed by washing.

RNA isolation and microarray analysis

Total RNA was isolated using a commercial kit from Qiagen. cDNA synthesis, hybridization to U74Av2 gene chips, chip processing, and data collection followed the manufacturer's instructions (Affymetrix Inc.).

Data analysis and statistics

Normalization and statistical analysis were done with GenePublisher v1.03 [10]. Affymetrix CEL files were uploaded to the GenePublisher server through http://www.cbs.dtu.dk/services/GenePublisher. All of the CEL files used in this study can be downloaded from http://zephyr.neuro.ki.se/*/Moliner_

CELfiles.zip. Gene tables obtained from GenePublisher were edited manually to eliminate entries with average signals lower than 50 and analysis of variance (ANOVA) p values higher than 0.05. For each entry, signals from triplicate chips were averaged, and the fold change was calculated relative to the corresponding values in either ES cells or 3-day or 8-day spheres. A cut-off of 50% fold change was arbitrarily chosen to define the set of genes that were differentially expressed between the three conditions. (Gene tables can be downloaded from http://zephyr.neuro.ki.se/*/Moliner_GeneTables.zip.) Gene set enrichment analysis (GSEA) was done with GSEA v2.0 [11] using unedited gene tables and the c2v2 gene set database (http://www.broad.mit.edu/gsea/msigdb/). The dataset was collapsed to gene symbols and 10,000 gene set permutations were performed for each binary comparison of phenotypes. As recommended by GSEA guidelines, only gene sets with an FDR q-value lower than 0.25 were taken into consideration; all other parameters were set to default values.

RESULTS

Neurogenic potential of spheres derived from mouse ES cells

Sphere colonies were derived from mouse ES cells essentially as described previously [4] except that to avoid the effects of retinol and possibly other components present in B27 supplement, N2 medium was used together
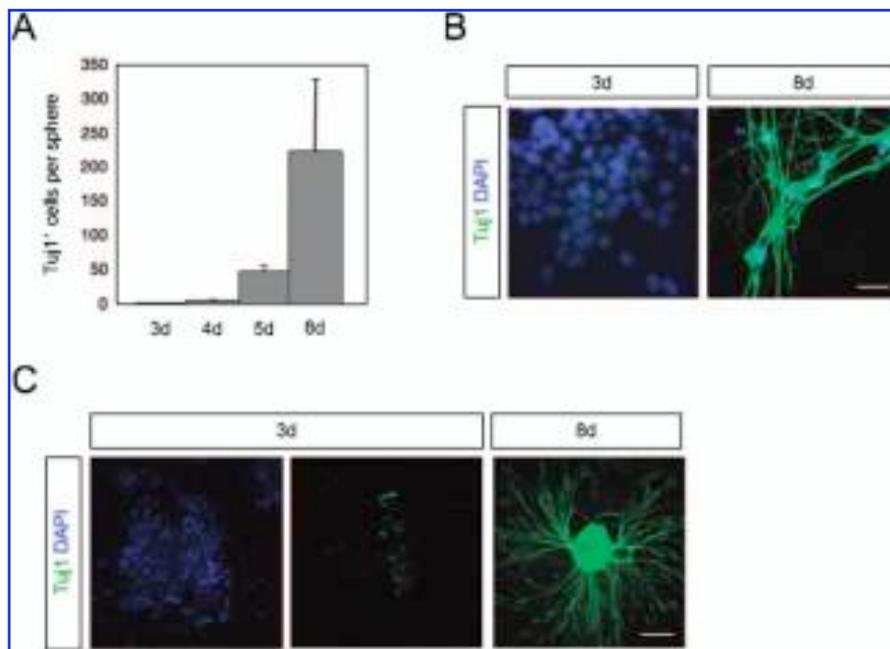
FIG. 2. Neuronal differentiation of ES cell-derived spheres. (**A**) Number of Tuj1$^+$ cells per sphere after 8d incubation in neuronal differentiation conditions. Results are presented as average $\pm$ SEM ($n = 3$). (**B**) Immunocytochemistry analysis of Tuj1 expression in 3d and 8d spheres derived from D3 ES cells. Cultures were counterstained with DAPI. Size bar, 25 μm. (**C**) Immunocytochemistry analysis of Tuj1 expression in 3d and 8d spheres derived from R1 ES cells. Day 3 cultures were counterstained with DAPI. Size bar, 100 μm.

with LIF and bFGF for the generation of sphere colonies. Three-day- and 8-day-old colonies derived from the D3 ES cell line retained expression of several stem cell markers characteristic of undifferentiated ES cells, including SSEA-1, Oct-3/4, and Sox2 (Fig. 1A). Flow cytometry analysis revealed that the vast majority of cells in 8-day-old spheres were positive for the stem cell marker SSEA-1 (93% ± 0.6, $n = 3$), indicating a very high proportion of undifferentiated stem cells in the spheres. Cell viability was also high (95.2% and 96.1% in 3-day- and 8-day-old spheres, respectively) as determined by Trypan Blue exclusion. Sphere colonies lacked expression of the neural stem cell markers Sox1, Sox3, and nestin (Fig. 1A). Nestin expression could only be observed after plating the spheres on an adherent substrate (Fig. 1B), suggesting a role for cell matrix attachment in NSC differentiation.

The neurogenic potential of spheres derived from D3 ES cells was assessed after plating sphere colonies in differentiation conditions for 8 days followed by staining with the Tuj1 antibody against the neuronal marker βIII-tubulin (see Materials and Methods). ES cell-derived spheres acquired neurogenic potential over several days of culture, indicating differences in neurogenic competence between different stages of sphere growth (Fig. 2A). In particular, 8-day-old (herein 8d) spheres produced many neurons upon withdrawal of LIF/bFGF and plating in differentiation conditions, whereas 3-day-old (3d) spheres produced none (Fig. 2B). Similar results were obtained when spheres derived from R1 ES cells were examined (Fig. 2C), indicating that this was a property common to several ES cell lines. Although 8d spheres contain 10–20 times more cells than 3d spheres, it was obvious from visual inspection of differentiation cultures that the neurogenic capacity of 8d cells could not be accounted for by differences in sphere cell content alone.

To investigate this further, we tested whether the neurogenic potential of 4d spheres could be elicited by either a prolonged period of differentiation (12 days instead of 8 days) or expansion prior to differentiation. Expansion was made by plating 4d spheres on coated dishes in sphere culture medium (i.e., with bFGF and LIF) during 4 days. In another experiment, the bone morphogenetic protein (BMP) inhibitor Noggin was added during expansion to cancel possible antineurogenic effects of endogenously produced BMP. However, none of these conditions resulted in any significant stimulation of neuronal differentiation that was comparable to that obtained with 8d spheres (Fig. 3A,B). As expected, neuronal differentiation of 8d cells was inhibited in the presence of BMP-2 (Figs. 3A,B). Together, these experiments indicate that factors or processes generated during prolonged sphere growth lead to the appearance of neurogenic competence in these cells.
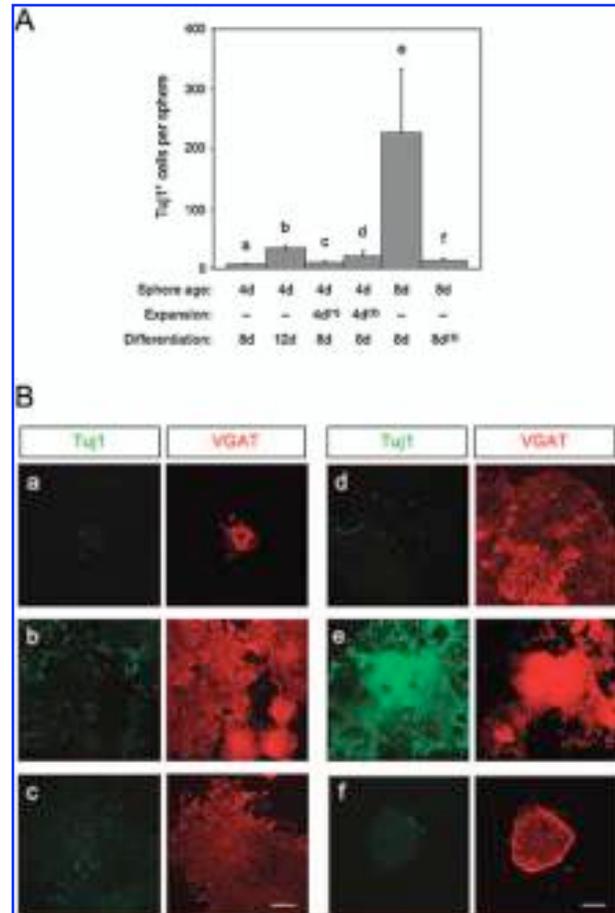
FIG. 3. Neurogenic competence in the sphere niche. (**A**) Number of Tuj1+ cells per sphere under the indicated conditions. [1] bFGF and LIF added during expansion. [2] bFGF, LIF, and noggin added during expansion. [3] BMP-2 added during the first 5 days of differentiation. Results are presented as average ± SEM ($n = 3$). (**B**) Immunocytochemistry analysis of Tuj1 expression (green) under the conditions indicated in **A**. Cultures were counterstained for the stem cell marker VGAT (red) [22]. Size bar, 100 μm.

Gene expression profiling of ES cell-derived spheres

To characterize the processes leading to neurogenic competence in ES cell-derived spheres, gene expression profiles were investigated in spheres derived from mouse R1 ES cells grown in N2 medium, bFGF, and LIF as described above. Figure 4A shows a schematic of the experimental design used for microarray analysis. Total RNA was isolated from four different cell populations: ES cells, 7-day-old first-generation spheres (7dP0), and 3-day- and 8-day-old passage 5 spheres (3dP5 and 8dP5, respectively). Prior to RNA extraction, ES cells were isolated free from MEF contamination, as previously described [3]. Triplicate RNA samples of each cell popu-

236
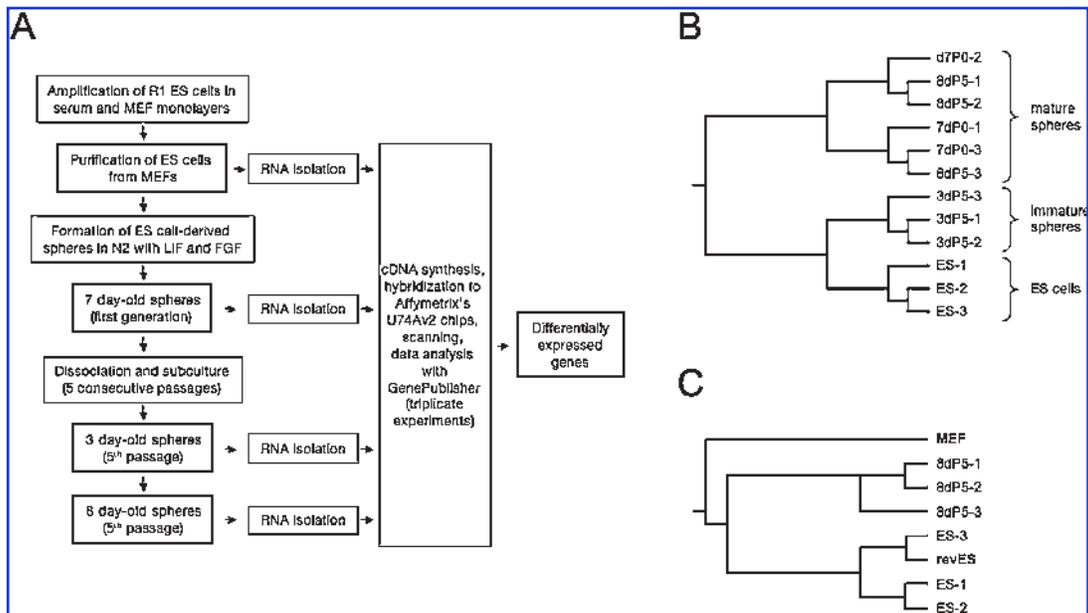
FIG. 4. Gene expression profiling of ES cell-derived spheres. (**A**) Schematic of the exprimental design of microrray experiments. (**B**) Hierarchical clustering of ES, 7dP0, 3dP5, and 8dP5 samples. (**C**) Hierarchical clustering of revES and MEF samples.

lation were obtained starting from three independent batches of mouse R1 ES cells. cDNA was hybridized to Affymetrix U74Av2 gene chips. Data normalization and statistical analysis were done using GenePublisher [10]. Hierarchical clustering using all of the genes showed that individual samples clustered together in the assigned categories, indicating reproducible differences between the samples analyzed (Fig. 4B). An informative exception was the mixed clustering of 7dP0 and 8dP5 samples, which indicated the absence of significant differences in gene expression between those two samples (Fig. 4B). This result suggests that gene expression patterns are maintained in equivalent stages of sphere development independently of passage number. This clustering also showed that the transcriptional profile of immature 3-day-old spheres is essentially intermediate between that of ES cells and mature spheres (Fig. 4B).

RNA was also extracted from MEF cells and used as a control for microarray analysis. Hierarchical clustering of the MEF results with those obtained in ES cells and spheres revealed a clear separation between the latter and MEF cells (Fig. 4C), indicating distinct gene expression profiles and thus negligible contamination with MEF material in the ES cell samples. In agreement with this, no overlap could be observed between the top scoring genes in the MEF and ES cell samples (not shown).

We also investigated the reversibility of the gene expression profile of mature, 8d spheres. To this end, cells dissociated from 8d spheres (5th passage) were plated under standard, adherent ES cell culture conditions, grown for three additional passages, and used for RNA extrac-

tion and microarray analysis. Hierarchical clustering showed a clear convergence between this sample (labeled revES) and ES cells (Fig. 4C), indicating no statistically significant differences between their gene expression profiles. Together, the results from these analyses show that sphere growth induces specific, reversible, and reproducible changes in the transcriptome of ES cells.

Single-gene analysis of expression profiles in ES cell-derived spheres

Affymetrix U74Av2 gene chips contain 12,488 different sequences from the mouse genome, although some genes are represented by more than one feature on this chip. Gene tables obtained with GenePublisher were edited manually to eliminate entries with average signals lower than 50 and ANOVA p values higher than 0.05. The fold change for each entry in the array was calculated for three different binary comparisons: (1) 3d spheres vs. ES cells; (2) 8d spheres vs. ES cells; and (3) 8d vs. 3d spheres. For each comparison, entries showing fold changes lower than 50% were removed, leaving a total of 200 genes showing statistically significant differences of 50% or greater in any of the three comparisons made. A total of 61 genes were found to be up-regulated and 64 down-regulated in 3d spheres compared to ES cells. In 8d spheres, 99 genes were found up-regulated and 67 down-regulated compared to ES cells. Finally, 26 genes were found to be up-regulated in 8d compared to 3d spheres, and none were significantly down-regulated by greater than 50%. Figure 5, A and B, shows Venn diagrams summarizing these results.
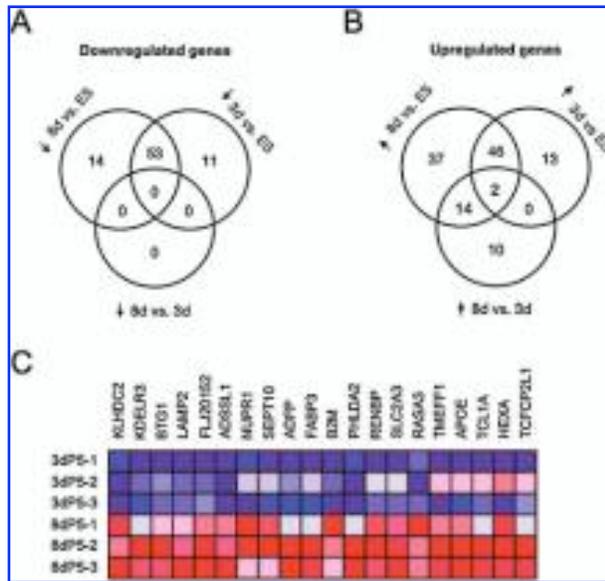
FIG. 5. Single-gene analysis of expression profiles in ES cell-derived spheres. (**A**) Venn diagram of down-regulated genes. (**B**) Venn diagram of up-regulated genes. (**C**) Heat map of genes up-regulated in 8d relative to 3d spheres.

The majority of gene down-regulations (64 out of 78 genes, or 82%) occurred during the first 3 days of sphere development (Fig. 5A). The fact that no significant gene down-regulations were detected when 8d spheres were compared to 3d spheres was also in agreement with this observation. In contrast, gene up-regulations took place more gradually during sphere growth, with approximately half occurring in 3d spheres (Fig. 5B). The 26 genes up-regulated in 8d relative to 3d spheres are listed in Table 1, and a heat map representation of the expression levels of a subset of these is shown in Fig. 5C. In this group, the expression of two genes, Acas2l and Apoe, was also found elevated in 3d spheres relative to ES cells, indicating a steady increase during sphere development, although the majority of these genes (14 genes) increased expression only during the last 5 days of sphere growth. The remaining 10 genes represented up-regulations in 8d spheres that had been preceded by a down-regulation in 3d spheres, resulting in no significant net change relative to ES cells.

The results of this analysis indicated that 3d spheres are transcriptionally at an intermediate state between ES cells and 8d spheres. However, as indicated above, only 8d spheres were capable of generating neurons when plated in differentiation conditions. Therefore, we selected 13 genes for further validation among those that appeared significantly up-regulated in 8d spheres relative to both 3d spheres and ES cells. Validation of microarray data was done by quantitative real-time RT-PCR (Q-PCR) on samples of total RNA that were different from

those used in the microarray experiments and obtained from independent cultures of ES cells and spheres. Changes in expression were averaged from two independent measurements and are indicated in Table 1. For most genes, higher fold increase values were obtained in the Q-PCR analysis than those observed in the microarray experiments, which is in agreement with observations made by other researchers and may have to do with the narrower dynamic range of DNA microarrays. Interestingly, the majority of the genes upregulated in 8d relative to 3d spheres have Gene Ontology annotations indicating functions in cell metabolism.

GSEA of expression profiles in ES cell-derived spheres

GSEA is a method for analysis of microarray data that extracts biological information by focusing on groups of genes that share a common biological function—so-called gene sets—rather than on single genes [11]. Because single-gene analyses center on fold changes above a certain threshold, modest increments in the expression of individual genes are usually neglected. If the relevant biological differences are modest relative to the noise inherent to microarray technology, very few individual genes may meet the threshold for statistical significance. However, small but concerted increments in a set of genes from a common pathway may have highly significant consequences for the function of that pathway and may be more biologically relevant than a large fold increase in a single gene. The GSEA method determines whether a rank-ordered list of genes for a particular comparison of interest (e.g., 8d vs. 3d spheres) is enriched in genes derived from independently generated gene sets. GSEA was applied to our data set using a molecular signature database curated from the biomedical literature that contains over 1,600 gene sets comprising different pathways, ontologies, chemical and genetic perturbations, clinical phenotypes and animal models (available from the GSEA Web site at http://www.broad.mit.edu/gsea/). This analysis revealed 40 and 45 gene sets significantly enriched in 3d and 8d spheres, respectively, compared to ES cells. In contrast, over 500 gene sets were found be depleted in 3d and 8d spheres relative to ES cells, indicating a wider down-regulation of pathways during sphere development. In addition, 68 gene sets were enriched and 24 depleted in 8d relative to 3d spheres, showing that GSEA was able to find both up- and down-regulation of pathways during the growth of 3d to 8d spheres.

Pathways enriched in 8d relative to 3d spheres could be ascribed to four main categories: mitochondrial function (particularly in ATP synthesis), cell metabolism, oxidative stress, and hypoxia (Table 2). Within the last category, three different gene sets up-regulated during

238

TABLE 1. LIST OF 26 GENES UP-REGULATED IN 8D RELATIVE TO 3D SPHERES[a]

ID	Gene symbol	Gene title	p	Fold array	Fold Q-PCR
94214_at	Fabp3	Fatty acid binding protein 3, muscle and heart	2.35E-02	2.97	3.90
104464_s_at	Kdelr3	KDEL (Lys-Asp-Glu-Leu) endoplasmic reticulum protein retention receptor 3	3.46E-02	2.97	5.68
160921_at	Acas21	Acetyl-coenzyme A synthetase 2 (AMP forming)-like	1.31E-02	2.10	—
95622_at	Klhdc2	Kelch domain containing 2	2.58E-02	2.00	—
93104_at	Btg1	B-cell translocation gene 1, anti-proliferative	2.50E-03	1.82	—
94206_at	Grcc10	Gene-rich cluster, C10 gene	1.16E-02	1.73	—
101590_at	Lamp2	Lysosomal membrane glycoprotein 2	1.47E-02	1.72	2.43
95518_at	FLJ20152	Hypothetical protein	4.94E-02	1.70	4.53
16129_f_at	Ppfibp2	Protein tyrosine phosphatase, receptor-type, F interacting protein, binding protein 2	2.01E-03	1.68	4.17
98435_at	Adssl1	Adenylosuccinate synthetase like 1	5.83E-03	1.68	—
160108_at	Nupr1	Nuclear protein 1	1.33E-02	1.66	10.80
161104_at	10-Sep	Septin 10	2.80E-02	1.64	—
93804_at	Slc2a3	Solute carrier family 2 (facilitated glucose transporter), member 3	9.79E-03	1.63	—
98589_at	Adfp	Adipose differentiation related protein	4.49E-02	1.63	—
92845_at	Oxct1	3-Oxoacid CoA transferase 1	1.10E-02	1.60	2.36
160472_r_at	Tmeff1	Transmembrane protein with EGF-like and two follistatin-like domains 1	3.95E-02	1.57	—
103761_at	Tcfcp211	Transcription factor CP2-like 1	8.59E-03	1.55	2.27
96154_at	Renbp	Renin binding protein	7.43E-03	1.54	5.06
93088	B2m	β2-microglobulin	2.27E-02	1.53	—
93026_at	Mgst1	Microsomal glutathione S-transferase 1	1.35E-03	1.53	—
97235_f_at	Apobec2	Apolipoprotein B editing complex 2	4.84E-02	1.52	1.91
104548_at	Phlda2	Pleckstrin homology-like domain, family A, member 2	9.14E-03	1.52	3.39
93296_at	Tcl1	T-cell lymphoma breakpoint 1	9.97E-03	1.51	3.49
94840_at	Hexa	Hexosaminidase A	8.24E-03	1.51	4.61
95356_at	Apoe	Apolipoprotein E	2.39E-03	1.50	—
93319_at	Rasa3	RAS p21 protein activator 3	2.55E-03	1.50	—

[a]Fold increases for 13 genes validated by qPCR are indicated.

hypoxia in a variety of cell types were enriched in 8d compared to 3d spheres. On the other hand, pathways depleted in 8d relative to 3d spheres (i.e., enriched in the latter compared to the former) included RNA transcription and processing, proteasome and myc pathways, and gene sets down-regulated by RA, oxidative stress, and hypoxia (Table 3). It is interesting to note that independent gene sets previously found to be up- and down-regulated by oxidative stress and hypoxia were, respectively, enriched and depleted in 8d compared to 3d spheres, strengthening the relevance of those pathways.

DISCUSSION

ES cell-derived spheres represent a novel and convenient way to grow and expand ES cells in the absence of serum and feeder cell layers [5]. As reported here, these cells acquire a reversible, proto-neurogenic potential during sphere growth. However, ES cell-derived spheres grown in N2 medium never expressed the NSC marker nestin, unless plated on an adherent surface (e.g., Fig. 1B), nor was nestin expression detected in our microarray experiments (A.M. and C.F.I., unpublished observations). This is in contrast to previously reported ES cell-derived sphere cultures grown with B27 supplement in which nestin expression was readily detected in the spheres themselves [4], a discrepancy that we attribute to the presence of retinol, which can be metabolized to RA, a potent neural inducer, and perhaps other components derived from B27 supplement. On the other hand, and unlike NSCs, the fact that ES cell-derived spheres retain stem cell status, as judged by SSEA-1 staining and pluripotency, indicates that the changes ES cells undergo

TABLE 2. GENE SETS ENRICHED IN 8D RELATIVE TO 3D SPHERES[a]

Pathway: gene set	Enriched/ total	Nominal p value	Core enrichment
Mitochondrial function			
APT synthesis	7/15	0.0001	ATP6V1G1, ATP6B0D1, ATP6V0B, APT6V1C1, ATP5E, ATP6V1B2
Oxidative phosphorylation	17/50	0.001	ATP6V1G1, APT6V0D1, ATP6V0B, SDHB, ATP6V1C1, ATP6V1H
Electron transport chain	21/71	0.004	NDUFA6, SDHB, SLC25A4, NDUFB9, NDUFA7, ATP5E, COX17
Fatty acid beta-oxidation	3/12	0.012	CPT1A, ACADL, ACSL1, ACADS, SLC25A20, ACADM, ACADVL
Cellular metabolism			
Valine and leucine metabolism	19/26	0.0001	ACAA2, ACADL, BCKDHB, MCCC1, HIBADH, MCEE, BCAT1
Propanoate metabolism	17/23	0.0001	SUCLG2, ACADL LDHB, MCEE, LDHC, ALDH1A1, ECHS1
TCA cycle	14/25	0.002	IDH2, SUCLG2, SDHB, IDH1, IDH3G, PCK1, SUCLA2, ACO2
Gluconeogenesis	19/39	0.006	PGM1, LDHB, PGK1, ALDOA, LDHC, PFKP, ALDH1A1, ALDH9A1
Cholesterol biosynthesis	5/14	0.01	SC4MOL, CYP51A1, HMGCS1, DHCR7, NSDHL
Sucrose metabolism	8/18	0.01	PGM1, UGDH, SI, ENPP1, PYGB, HK2, AGL, HK1
Tryptophan metabolism	16/29	0.012	CYP51A1, CAT, AOX1, DDC, ALDH1A1, ECKS1, ALDH9A1
Fatty acid metabolism	10/48	0.013	ACAA2, ASAH1, SC4MOL, CPT1A, ACADL, CYP51A1, ACSL1
Butanoate metabolism	13/19	0.024	SDHB, ALDH1A1, ECHS1, GAD1, ALDH9A1, PDHA1, ACAT2
Oxidative stress (induced)			
Stress arsenic specific	32/100	0.0001	ADFP, PLTP, ASNS, HEXA, ATP6V1G1, ATP6V0D1, SERPINH1
Hypoxia (induced)			
Hypoxia fibro up	10/20	0.015	ADFP, AMPD3, ALDOA, PFKP, F3, BACH1, BAPX1, ALDOC, VEGF
Mense hypoxia up	20/63	0.001	ADFP, SLC2A3, RORA, WSB1, BHLHB2, PGK1, ELL2, CEBPB
Hypoxia reg up	8/33	0.017	ADFP, CCNG2, DUSP1, BHLHB2, PGK1, ALDOA, PFKP, F3

[a]For each gene set, the number of enriched versus total genes and nominal p value are indicated. A subset of the genes that contribute most to the enrichment result is listed under the "Core enrichment" heading.

during sphere growth do not involve an irreversible commitment to a particular phenotype. This reversibility also suggests moderate biological differences, which is in agreement with the relatively modest number of genes that were found to be significantly altered by greater than 50% between ES cells and 3d or 8d ES cell-derived spheres (125 and 166 genes, respectively). This is in contrast to earlier studies that compared gene expression profiles between ES cells and NSCs isolated from the mouse brain, in which anything from 666 [1] to 2,580 [2] differentially expressed genes were identified using comparable thresholds. From these earlier studies, our results are probably more comparable to the estimate made by D'Amour et al., which is also likely to be the most relevant, as these authors compared transcriptional profiles of ES cells and the NSC progeny derived from the same cells isolated from chimeric fetuses, eliminating the variability that arises from genomic heterogeneity [1].

Comparisons of individual genes as well as GSEA indicated a relatively rapid, i.e., within the first 3 days, and broad down-regulation of genes and pathways upon growth of ES cell-derived spheres. This could reflect a reduced level of plasticity in sphere cells. In contrast, up-regulation of genes and pathways occurred mostly progressively and/or during later stages of sphere development. Interestingly, the majority of the differences in individual genes or pathways observed between 3d and 8d spheres (both up- and down-regulations) were not preceded by significant changes in expression between ES cells and 3d spheres. Together, these observations indicate that distinct types of changes take place during the initial growth of ES cells to 3d spheres and then from 3d to 8d spheres, and suggest the existence of qualitative differences between these three stages.

The list of the 26 most up-regulated genes in 8d relative to 3d spheres contains many genes of still unknown function and did not reveal any obvious functional bias, with the possible exception of genes encoding products with functions in cell metabolism. However, subsequent analyses of gene set enrichment using the GSEA algorithm revealed, in addition to alterations in metabolic pathways, significant changes in mitochondrial function, particularly ATP synthesis, RNA transcription and proteasomal machineries, and pathways activated in response to oxidative stress and hypoxia, and controlled by

TABLE 3. GENE SETS ENRICHED IN 3D RELATIVE TO 8D SPHERES

Pathway: gene set	Enriched/ total	Nominal p-value	Top core enrichment
mRNA metabolism			
RNA polymerase	7/12	0.001	POLR2J, POLR2D, POLR2I, POLR2L, POLR2K, POLR2F
mRNA processing	17/31	0.003	SFRS7, U2AF2, SF3A3, FUSIP1, HNRPR, LSM3, PRPF8, SFRS1
mRNA splicing	18/32	0.002	SFRS7, SF3A3, PPAN, SRP19, PPIG, PRPF8, SHRPB, SMNDC1
mRNA processing reactome	12/25	0.001	SFRS7, BRUNOL4, U2AF2, NCBP2, SF3A3, FUS, FUSIP1
RNA transcription reactome	21/71	0.009	POLR2J, POLR2I, POLR2K, POLR2F, POLR1A, POLR2H
Proteasome pathway			
Proteasome	12/17	0.005	PSMA5, PSMB10, PSMA7, PSMA6, PSMB7, PSMA2, PSMB8
Proteasome pathway	15/21	0.007	UBE2A, PSMA5, PSMA7, PSMD14, PSMA6, PSMB7, PSMA2
Oxidative stress (repressed)			
AS3 Fibro C4	7/14	0.001	MYCN, F11R, GRB2, TAPBP, JUN, MAP3K8, NR2F6
Hypoxia (repressed)			
Manalo hypoxia dn	30/71	0.0001	PPARD, MAD2L1, MRPL40, PSME3, PA2G4, GTPBP4, MRPS12
Myc pathway			
Myc targets	14/38	0.005	MYC, SRM, NME1, FASN, CDKN2B, CAD, APEX1, TP53, HSPA4
Retinoic acid (repressed)			
Xu atra plusnsc dn	7/15	0.0001	MYC, DDX10, RUVBL2, EIF3S9, CSE1L, DDX18, PPM1G

[a]For each gene set, the number of enriched versus total genes and nominal p value are indicated. A subset of the genes that contribute most to the enrichment result is listed under the "Core enrichment."

myc and RA. It is interesting that development of 8d spheres appears associated with down-regulation of a gene set that is normally down-regulated by RA, because it suggests that sphere growth mimics some of the transcriptional effects induced by treatment with a well-known neural-inducing agent. It is also interesting to note a relative depletion in the expression of gene sets comprising *myc* genes and myc targets in 8d compared to 3d spheres. Down-regulation of myc-regulated pathways, particularly N-myc, has previously been associated with reduced proliferation of neural progenitors and ectopic formation of neurons [12].

Several gene sets related to cell metabolic functions were also found enriched in 8d compared to 3d spheres. Prominent among these were a number of sets encoding products with functions in intermediate metabolism, including glycolysis, the tricarboxylic acid (TCA) cycle, and adenosine triphosphate (ATP) synthesis, suggesting that increased energy requirements may be associated with sphere growth and neurogenic competence. An increased metabolic demand in 8d spheres is also suggested by the enrichment in gene sets related to cholesterol biosynthesis and metabolism of various amino acids, fatty acids, and intermediate metabolites. Two gene sets associated with components of the proteasome machinery were found to be depleted in 8d relative to 3d spheres. Reduced proteasome function has been linked to in-

creased neuronal differentiation in embryonic carcinoma cells [13], suggesting that lower proteasome activity may favorably influence neurogenesis. Recent studies have also established a link between oxidative stress and neuronal differentiation. Resistance to oxidative stress accompanied increased survival and neuronal differentiation of NSCs [14], and the cellular redox state regulated responsiveness to stimuli that promote differentiation of neuronal cell lines [15,16], indicating the importance of oxidative stress responses in the regulation of neural stem cell survival and neuronal differentiation.

Although standard conditions for mammalian cell culture are adjusted to reflect mammalian body temperature and CO_2 venous concentrations, they are not adjusted to normal physiological O_2 levels, which in the mammalian brain are approximately one order of magnitude lower than in a standard cell culture incubator [17]. This realization has prompted several researchers to investigate the impact of lower O_2 levels on neural precursor proliferation and neuronal differentiation. The bulk of this work has led to the conclusion that hypoxic conditions stimulate neurogenesis both in vitro [17,18] and in vivo [19,20]. Thus, it is interesting to note that growth of 3d to 8d spheres was associated with enrichment in three independent gene sets that are up-regulated upon hypoxia in different cell types, and depletion of a fourth one that has been found to be down-regulated by hy-

poxia. ES cell-derived spheres grow significantly in size from 3d to 8d (from 10–20 to about 200 cells, respectively), so it is conceivable that this growth sets constraints on O_2 transport toward cells in the middle of the sphere, leading to hypoxic conditions in the sphere center. Interestingly, vascular endothelial growth factor (VEGF), one of the genes contributing to the enrichment of the Hypoxia_fibro_up gene set in 8d spheres, has been found to stimulate expansion of NSCs in vitro and neurogenesis in vivo [21].

In conclusion, we have identified several genes and pathways that may underlie some of the early transitional stages between ES and neural stem cells. Some of these may represent useful markers for future studies of NSC development. The identification of candidate pathways by gene set enrichment analysis has allowed us to formulate hypotheses about events that may be important for the development of neurogenic competence in a stem cell niche that can now be tested using ES cell-derived spheres or other cellular models.

ACKNOWLEDGMENTS

REFERENCES

1. D'Amour KA and FH Gage. (2003). Genetic and functional differences between multipotent neural and pluripotent embryonic stem cells. Proc Natl Acad Sci USA 1: 11866–11872.

2. Ivanova NB, JT Dimos, C Schaniel, JA Hackney, KA Moore and IR Lemischka. (2002). A stem cell molecular signature. Science 298:601–604.

3. Ramalho-Santos M, S Yoon, Y Matsuzaki, RC Mulligan and DA Melton. (2002). "Stemness": transcriptional profiling of embryonic and adult stem cells. Science 298:597–600.

4. Tropepe V, S Hitoshi, C Sirard, TW Mak, J Rossant and D van der Kooy. (2001). Direct neural fate specification from embryonic stem cells: a primitive mammalian neural stem cell stage acquired through a default mechanism. Neuron 30:65–78.

5. Andäng M, A Moliner, CF Ibáñez and P Ernfors. (2007). Rapid and robust mouse ES cell culture system in fully defined medium (submitted).

6. Hitoshi S, RM Seaberg, C Koscik, T Alexson, S Kusunoki, I Kanazawa, S Tsuji and D van der Kooy. (2004). Primitive neural stem cells from the mammalian epiblast differentiate to definitive neural stem cells under the control of Notch signaling. Genes Dev 18:1806–1811.

7. Fedoroff S and A Richardson. (2001). In Protocols for Neural Cell Culture, 3rd ed. Humana, Totowa, NJ, 362 pp.

8. Lane MA, AC Chen, SD Roman, F Derguini and LJ Gudas. (1999). Removal of LIF (leukemia inhibitory factor) results in increased vitamin A (retinol) metabolism to 4-oxoretinol in embryonic stem cells. Proc Natl Acad Sci USA 96:13524–13529.

9. Castro-Obregon S and L Covarrubias. (1996). Role of retinoic acid and oxidative stress in embryonic stem cell death and neuronal differentiation. FEBS Lett 381:93–97.

10. Knudsen S, C Workman, T Sicheritz-Ponten and C Friis. (2003). GenePublisher: Automated analysis of DNA microarray data. Nucleic Acids Res 31:3471–3476.

11. Subramanian A, P Tamayo, VK Mootha, S Mukherjee, BL Ebert, MA Gillette, A Paulovich, SL Pomeroy, TR Golub, ES Lander and JP Mesirov. (2005). Gene set enrichment analysis: a knowledge-based approach for interpreting genome-wide expression profiles. Proc Natl Acad Sci USA 102:15545–15550.

12. Knoepfler PS, PF Cheng and RN Eisenman. (2002). N-myc is essential during neurogenesis for the rapid expansion of progenitor cell populations and the inhibition of neuronal differentiation. Genes Dev 16:2699–2712.

13. Baldassarre G, A Boccia, P Bruni, C Sandomenico, MV Barone, S Pepe, T Angrisano, B Belletti, ML Motti, A Fusco and G Viglietto. (2000). Retinoic acid induces neuronal differentiation of embryonal carcinoma cells by reducing proteasome-dependent proteolysis of the cyclin-dependent inhibitor p27. Cell Growth Differ 11:517–526.

14. Sousa KM, H Mira, AC Hall, L Jansson-Sjostrand, M Kusakabe and E Arenas. (2007). Microarray analyses support a role for nurr1 in resistance to oxidative stress and neuronal differentiation in neural stem cells. Stem Cells 25:511–519.

15. Kamata H, S Oka, Y Shibukawa, J Kakuta and H Hirata. (2005). Redox regulation of nerve growth factor-induced neuronal differentiation of PC12 cells through modulation of the nerve growth factor receptor, TrkA. Arch Biochem Biophys 434:16–25.

16. Masutani H, J Bai, YC Kim and J Yodoi. (2004). Thioredoxin as a neurotrophic cofactor and an important regulator of neuroprotection. Mol Neurobiol 29:229–242.

17. Studer L, M Csete, SH Lee, N Kabbani, J Walikonis, B Wold and R McKay. (2000). Enhanced proliferation, survival, and dopaminergic differentiation of CNS precursors in lowered oxygen. J Neurosci 20:7377–7383.

18. Morrison SJ, M Csete, AK Groves, W Melega, B Wold and DJ Anderson. (2000). Culture in reduced levels of oxygen promotes clonogenic sympathoadrenal differentiation by isolated neural crest stem cells. J Neurosci 20:7370–7376.

19. Zhu LL, T Zhao, HS Li, H Zhao, LY Wu, AS Ding, WH Fan and M Fan. (2005). Neurogenesis in the adult rat brain after intermittent hypoxia. Brain Res 7:1–2.

20. Fagel DM, Y Ganat, J Silbereis, T Ebbitt, W Stewart, H Zhang, LR Ment and FM Vaccarino. (2006). Cortical neurogenesis enhanced by chronic perinatal hypoxia. Exp Neurol 199:77–91.

21. Schanzer A, FP Wachs, D Wilhelm, T Acker, C Cooper-Kuhn, H Beck, J Winkler, L Aigner, KH Plate and HG Kuhn. (2004). Direct stimulation of adult neural stem cells in vitro and neurogenesis in vivo by vascular endothelial growth factor. Brain Pathol 14:237–248.

22. Andäng M, J Hjerling-Leffler, A Moliner, TK Lundgren, G Castelo-Branco, E Nanou, E Pozas, V Bryja, S Halliez, H Nishimaru, J Wilbertz, E Arenas, M Koltzenburg, P Charnay, A El Manira, CF Ibáñez and P Ernfors. (2007). Histone H2AX-dependent GABAA receptor regulation of stem cell proliferation. Nature 451:460–464.

Address reprint requests to:
Dr. Carlos F. Ibanez
Department of Neuroscience
Karolinska Institute
17177 Stockholm, Sweden

E-mail: carlos.ibanez@ki.se